SCIPP 97/04
March 1997

Silicon Microstrip Detectors in High Luminosity Application

Hartmut F.-W. Sadrozinski

SCIPP, University of California Santa Cruz, Santa Cruz, CA 95064

Abstract

The development of silicon microstrip detectors for high luminosity application at the Large Hadron Collider (LHC) is described. The technical choices are most severely restricted by the anticipated radiation damage. The arguments are presented which led to the selection of the base line detectors for the silicon tracker of the LHC detector ATLAS: sandwiches of single-sided detectors of n-strips in n-type bulk.

1. INTRODUCTION

The advent of high luminosity colliders requires special instrumentation in High Energy Physics [L1-L3]. High rates can lead to a pile-up of events and increased dead time. For the readout electronics, this means the use of much shorter shaping times than one would use to optimize the power consumption and the signal-to-noise ratio. In addition, most detectors have be subdivided into many more channels to reduce the confusion of signals. A new problem at the hadron colliders is the increased radiation levels. Already at the Main injector upgrade at FNAL and even more so at the Large Hadron Collider, radiation damage dictates compromises in many detector subsystems. This applies especially to semiconductor detectors, which, due to their relatively high cost and extremely good position resolution are commonly employed close to the interaction region where the radiation levels are highest.

As described below in detail, the layout of tracking devices based on silicon detectors is severely constrained: they have to be located such that they can survive the radiation for the life time of the experiment [T1, T2]. In the same context, a silicon tracking detector which is more radiation hard allows the detectors to be moved closer to the interaction region, improving the performance in vertexing and momentum resolution and reducing the area of the tracker, and therefore the cost. Thus it is not surprising that the silicon strip detectors developed for ATLAS SemiConductor Tracker (SCT) [T2] are different then the ones developed for low-luminosity applications such as LEP [T4] or even BaBar [T5], where only ionizing radiation is present.

In this report, the basic functioning of silicon microstrips will be explained first, followed by discussion of radiation damage in silicon detectors. The layout of the ATLAS SCT will be

presented, and design features of the detectors highlighted which are specific to the operating conditions at the LHC. The projected performance of both irradiated and non-irradiated detectors will be detailed, based on beam test measurements.

2. BASICS of SILICON MICROSTRIP DETECTORS [Refs. D1-D3]

Silicon detectors are made from near intrinsic bulk having both low-ohmic donor implants (the n-side), collecting electrons, and low-ohmic acceptor implants (the p-side), collecting holes. The n-side signal is mainly due to drifting electrons collected in ~8ns, (for the usual 300 μm thickness and with bias above the depletion voltage). The p-side signal is mainly due to drifting holes with a three times longer collection time, due to the larger mobility. One side has a junction, the other is ohmic. The location of the junction depends on the type of the bulk: it is on the p-side in n-bulk and the n-side in p-bulk. Charge is collected only from the depleted region, which starts at the junction side when the bias voltage is raised from zero, and reaches the full thickness of the detector at the depletion voltage. Single-sided detectors have only one side divided into strips which are read out, double-sided detectors have both sides divided into read-out strips. Most (all?) silicon detectors are made of high-ohmic n-bulk with resistivity of about 5 kΩ-cm, determined by a small fraction (10^{12} per cm^3) of donor atoms. The distance between strip centers, the pitch, is of the order of 50 μm, and thus of the same order of magnitude as the feature size of VLSI chips. This has facilitated the development of read-out electronics which is directly wire-bonded to the strips and helps in the data compression of the large number of channels [E1-E9].

The original single-sided detectors had the p strips implanted in n-bulk and coupled directly to the read-out electronics. Later, AC-coupling was developed which decoupled the DC current and the biasing potential from the front-end electronics. This made the use of double-sided detectors feasible, which are an economical and low-mass technical choice [D2]. Yet, the LHC experiment ATLAS has chosen as the baseline a sandwich of single-sided detectors with n-implants in n-bulk, glued back-to-back. The reason is the expectation that they will present better performance after severe radiation damage predicted for LHC operations.

3. RADIATION DAMAGE in SILICON STRIP DETECTORS [Refs. R1-R8]

3.1 Surface Damage [Refs. S1-S6]

Ionizing radiation deposits charges on the surface of silicon strip detectors, which change their electrical properties. The processing of the surface, and the existence of oxides or nitrides can be a factor in the extent and consequences of the damage. When exceedingly large dose rates where used, increased leakage currents were observed due to charge-up of the surface, which annealed out in less then an hour at room temperature [E3, R7]. These effects are difficult to

quantify and we have dealt with them by performing a beam test at particle fluxes and operating temperatures anticipated for the LHC (see Sec. 5)

A more lasting damage to the surface is due to the accumulation of charges in the interface between the silicon oxides and the silicon bulk, where there is a lattice mismatch. The interface states are filled in ionizing radiation and saturate after a total dose of the order of 100 kRad [S1]. The important detector parameters which can be influenced by the existence of these oxide charges are bias resistance, inter-strip resistance and inter-strip capacitance.

Polysilicon bias resistors are radiation hard [S1], while those using an accumulation layer or the punch-through effect are changed drastically with radiation [S3, S6]. Moreover, the punch-through resistors introduce excess noise [S6, R7].

The inter-strip resistance is crucial for the isolation of the strips, and has to be much larger than the biasing resistor. The isolation is a problem on the n-side (ohmic side) before radiation due to the existence of a conducting accumulation layer of electrons below the normal oxide charges, but can be cured by implanting p-material as isolation ("p-stops") [D2]. After irradiation, when the bulk inverts [see below] and the junction is on the n-side, this problem vanishes. The p-side in turn does not have the accumulation layer after inversion and has good isolation.

The inter-strip capacitance is important because it tends to be the largest contributor to the parasitic capacitance responsible for amplifier noise. In the absence of free charges, it can be estimated fairly reliably from the geometry of the strip detector and is a function of the ratio strip width over strip pitch [C1-C4]. The existence of free charges on the n-side before inversion causes the capacitance to depend on the bias voltage and one reaches the minimum "geometrical" value only with large over-voltage.

Surface currents due to the oxide charges have been observed, but they are much less important than the bulk currents for charged particle radiation [S1, S4, S5].

3.2 Bulk Damage [Refs. I1, A1-A3]

The bulk is damaged mainly by displacement ["Non-ionizing Energy Loss" (NIEL)] [F1]. Hence hadrons and heavy ions damage more than electrons and photons. Two major effects are observed: an increase in leakage current due to the creation of deep acceptor levels and a change in the depletion voltage due to the change in effective doping concentration.

a) Increase in Leakage Current

The leakage current is due to a thermal generation of electron-hole pairs. It varies exponentially with the operating temperature. Due to the creation of deep traps which occupy the middle of the band gap [R8], radiation increases the leakage current i proportionally with the displacing fluence ϕ and the volume Vol

$$i = \alpha \cdot \phi \cdot Vol,$$

with $\alpha \approx 3*10^{-17}$A/cm after annealing. A large part of the current seems process dependent, but anneals out very fast. The leakage current is the reason why AC coupled detectors are used, which block the current from the amplifier input. But it also causes stochastic noise in the amplifier, proportional to the square root of the product of leakage current and shaping time. The allowable current limit for fast shaping times is about one μA per strip.

b) Change in Depletion Voltage [Ref. I1]

The depletion voltage V_{dep} depends on the effective doping concentration N_{eff} and the square of the detector thickness d:

$$V_{dep} = \frac{e \cdot |N_{eff}| \cdot d^2}{2 \cdot \varepsilon} \quad .$$

Thus a radiation induced change in the doping concentration causes a change in the depletion voltage [I1]. The effective doping concentration is changed in two ways: donor removal and acceptor creation, and both make the bulk more p-type. The donor removal is exponential, while the acceptor creation is linear in the fluence ϕ [Fig. 1]

$$N_{eff} = N_0 e^{-c\phi} + \beta\phi \quad .$$

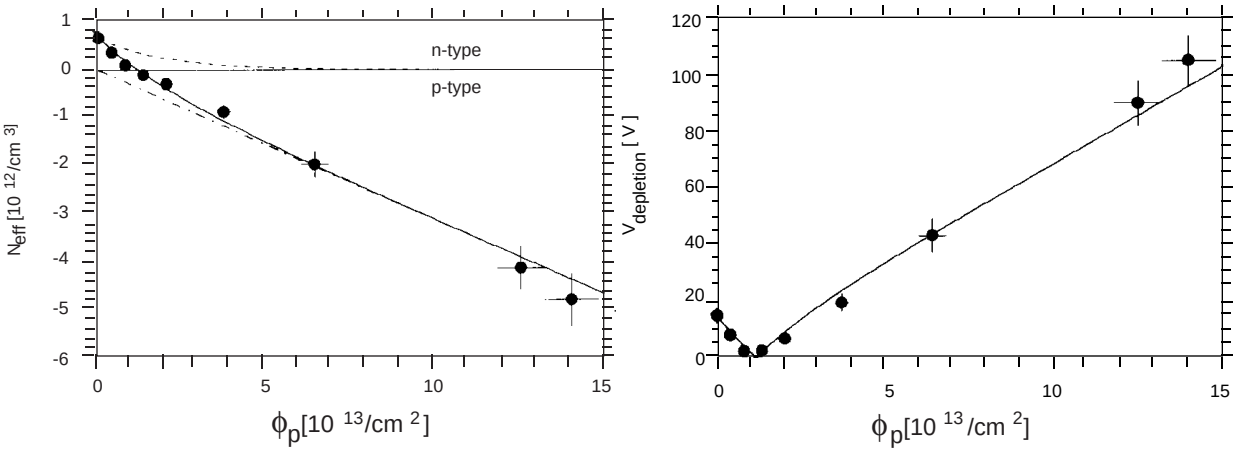

Fig. 1 Radiation damage in a 170μm thick n-bulk photo diode as a function of proton fluence ϕ_p:
a) effective doping density, b) depletion voltage (Ref. I1). For 300 μm thick detectors, the depletion voltages would be about three times as high.

At a certain fluence, about $\phi = 1*10^{13}$p/cm^2 in Fig. 1, the remaining donors are balanced by the newly created acceptors and the detector is intrinsic with zero depletion voltage. For larger fluences, the acceptors dominate and the detector is inverted, *i.e.* p-type, and the detector is said to have undergone "type inversion". For large fluences, the depletion voltage increases linearly with fluence, and is independent of the pre-rad value.

c) Annealing [Refs. A1-A3]

The radiation induced changes in detector properties are initially not stable, but exhibit strong annealing, which is temperature dependent. This means that the increased leakage currents and the modified doping concentration change even after the irradiation has finished. For example, at room temperature, the leakage currents decrease by about a factor of two in a few weeks. The annealing of the doping concentration is more complicated: there are three different effects with different time constants: there is first a constant term; then a short term annealing governed by τ_S, which is beneficial because it reduces the depletion voltage; and a long-term reverse- ("anti") annealing effect due to the release of meta-stable acceptors, which increases the depletion voltage with a characteristic time τ_L. Fig. 2 shows the depletion voltage both during irradiation and annealing for two different operating temperatures.

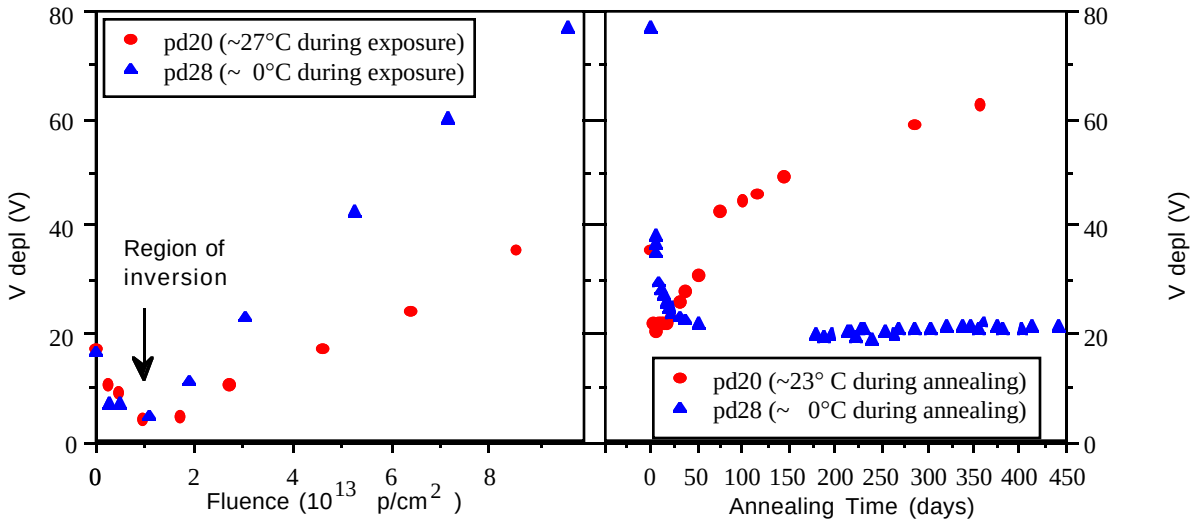

Fig. 2 The depletion voltage of 170 µm thick Hamamatsu photo-diodes as a function of fluence and as a function of annealing time for 0°C and room temperature operation. The last points on the left hand plot correspond to the first points on the right hand plot. (Ref. A1)

In good approximation for the fluences at the LHC, the three components, stable, short-term, and long-term annealed, respectively, are proportional to the fluence ϕ

$$V_{dep} = \phi[v_z + v_s e^{-t/\tau_s} + v_s(1 - e^{-t/\tau_L})] \quad .$$

The annealing times are both exponential functions of the temperature and the long annealing time τ_L is about 200 times longer than the short anneal time τ_S. After a fluence of $\phi = 1*10^{14}$p/cm^2, a typical fluence for 10 years of LHC operation, the constant term in the depletion voltage is about 100V, the short-term annealing term is about 300V and the reverse annealing term is also 300V. Thus, depending on the operating temperature, the depletion voltage can vary between 100V and 400V! This is illustrated in Fig. 3, where the depletion voltage for different detectors irradiated to the same fluence of about $5*10^{13}$p/cm^2, but annealed out at different

temperatures is shown: the detectors annealed out at elevated temperatures are reverse-annealed out completely to about 230V, while the detectors operated at 0^{o}C or below are still in the first phase of short-term annealing.

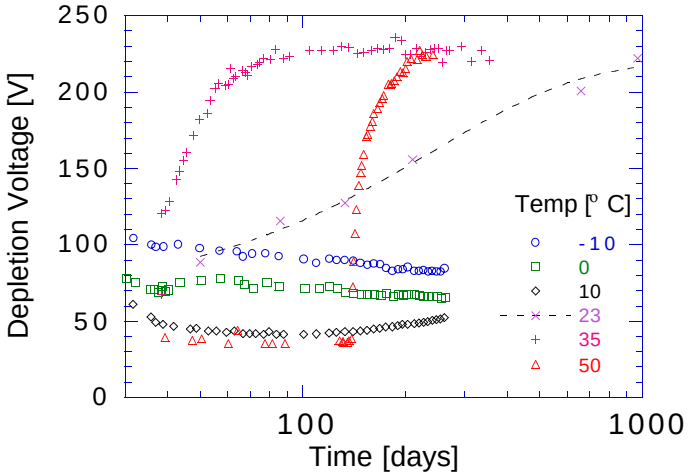

Fig. 3 Temperature dependence of the annealing of the depletion voltage for photo diodes irradiated with about $5*10^{13}$ p/cm^2. The detector at 50 ^{o}C was kept at -20^{o}C until day 140. (Ref. A1)

d) Consequences for the Operation of Silicon Detectors

In order to conserve power, and for safe operation, the depletion voltage should be kept as low as possible. Over the lifetime of the detectors at LHC, the detectors will be subjected to fluences in excess of 10^{14}p/cm^2. The depletion voltage will change from the initial pre-rad value of about 50V to zero to a final value which depends both on the fluence and the operating temperature. Type inversion (see above) occurs at a fluence of about 10^{13}p/cm^2 , i.e., after one year at full LHC luminosity. Given that the damage constants are proportional to the fluence received by the detector, the only additional parameter which controls the depletion voltage is the operating temperature. It has to be kept low to prevent the reverse annealing, but to allow the short-term annealing to take place during the lifetime t of the detector:

$$\tau_S << t << \tau_L \ .$$

For the life time of the LHC detectors of about t = 10 years, this corresponds to an operating temperature between -5 and -10^{o}C [R3]. Access scenarios which result in warm-up of the irradiated detectors have to be evaluated carefully. For example, warming up the detectors every year for 7 days from -10^{o} to +20^{o}C , instead of keeping the operating temperature constant at -10^{o}C, will increase the depletion voltage by 40% .

As mentioned before, the leakage current is a noise source. Short shaping times are required, in addition to the low temperature to minimize the current [E2]. The leakage current

produces heat, which has to be removed. Due to the exponential temperature dependence of the leakage current, the self-heating has to be controlled carefully in order to avoid thermal run-away, which puts severe requirements on the cooling system (see below) [H1].

It should be noted that there have been investigations using different bulk materials. One idea was to use p-material, with n-implants. It has the advantage that there is no inversion during the detector life time due to radiation damage: the junction stays on the n-side, and the quality control of the detectors is simplified [Z1]. Unfortunately, there is much less experience with p-bulk processing and more importantly, the radiation damage constants for p-bulk are not much different than for n-bulk [R4, R5]. Another idea was to use lower resistivity n-bulk material for the detector, which increases the initial pre-rad depletion voltage and shifts the inversion point to higher fluences [R1]. Given that the depletion voltage at very large fluences is determined by acceptor creation and not by the removal of donors, the ultimate depletion voltage is the same for both high- and low-ohmic material.

4. DESIGN and LAYOUT of the ATLAS SCT DETECTORS [Refs. T1, T2]

Uncertainties in predicting the dose and operating temperature require that the detectors be designed with "head room", *i.e.*, enough margin in performance to minimize degradation due to unforeseen conditions. Although there has been many years of experience with silicon detectors for example at LEP [T4], detectors have been used in high rate and high radiation environment only in the SVX at the FNAL Collider [S6] and the LPS at HERA [E3].

The ATLAS SCT chose a sandwich of single-sided n-on-n detectors as the base line, instead of double-sided detectors. Figure 4 shows the main features: two 6 cm x 6 cm detectors are bonded together to make 12 cm read-out strips and are then glued back-to-back with another 12 cm long pair, with a 40 mrad stereo angle. The electronic readout is straddling the center of the module, to minimize the noise contribution from the strip resistance [N2]. The pitch of the detectors is 80 μm, with narrow (≈ 16 μm wide) implants to minimize the inter-strip capacitance [C2, C4].

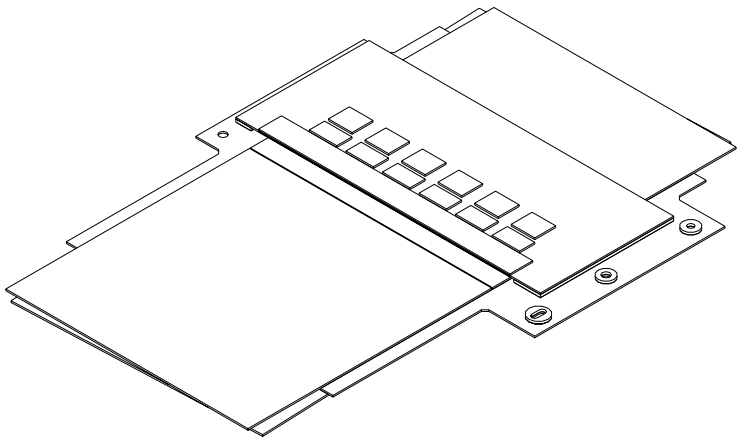

Fig. 4 The ATLAS SCT silicon module consisting of pairs silicon detectors glued together back-to-back.

A certain amount of conservatism should be applied when extrapolating the finding of short-term R&D to detector designs which will be operated for 10 years in ATLAS. The prediction [Refs. F1-F4] for the depletion voltage for the innermost SCT layer at 30 cm radius varies from 150V to 250V, depending on the assumptions. In the forward region, the expected values are between 300V and 500V. There is considerable uncertainty in the depletion voltage prediction, depending on assumption made for the radiation history and the operating temperature of the detectors. If one requires that the detector be efficient for a depletion voltage after inversion of 300V and that it can function with reduced performance with twice the depletion voltage at the same bias voltage, one is led to using single-sided detectors with n-side read-out. The reasoning is given in detail in the following.

4.1 Charge Collection [Refs. U1-U4, R7]

The signal collection is well understood before irradiation. The signal charge is proportional to the width of the depleted region. Aside from surface effects, the width of the depleted region x depends on the ratio of the bias voltage to the depletion voltage

$$x = d * \sqrt{\frac{V_{bias}}{V_{dep}}} \quad , \quad V_{bias} < V_{dep}$$

$$x = d \quad , \quad V_{bias} \geq V_{dep}$$

,

where d is the detector thickness. Biased above depletion, the only difference between the p- and n-sides is the longer collection time of the holes, which can cause a ballistic deficit at fast shaping times and small over voltage [E2]. Biased below depletion, the signal collection depends on whether the collection happens on the junction side or on the ohmic side. On the junction side, the signal charge is collected on one or two strips. On the ohmic side, the strips are shorted out and the charge is collected on many strips. Consequently, the efficiency for detecting tracks on the ohmic side is much reduced if operated below depletion (Fig. 5a). Before irradiation, the depletion voltage is between 50V and 100V and the detectors can easily be biased above depletion. This is the reason why in the past, in low radiation application, p-on-n or double-sided detectors were used almost exclusively and why they constitute the basis of our operating experience.

The signal collection after irradiation is well measured: first there is signal loss due to charge trapping. Measurements have shown that the loss of charge due to trapping is of the order 15% at the highest LHC fluences considered [R6]. At a fluence of about 10^{13}p/cm^2 (~1/10 of the total life time for the ATLAS SCT) the bulk inverts from n-type to p-type. The junction moves to the n-side. As before irradiation, the charge collection on the junction side is efficient even below depletion (Fig. 5b). The p-side becomes the ohmic side, and below depletion, the

generated charge is collected on several strips, as before irradiation, although they are not shorted out. Hence, for irradiated detectors, operation close to depletion is required for the p-side, while operation below depletion is possible for the n-side. The n-side exhibits good efficiency >95% when biased at 50% of depletion voltage, while the p-side shows good efficiency only when biased above depletion voltage (Fig. 5b).

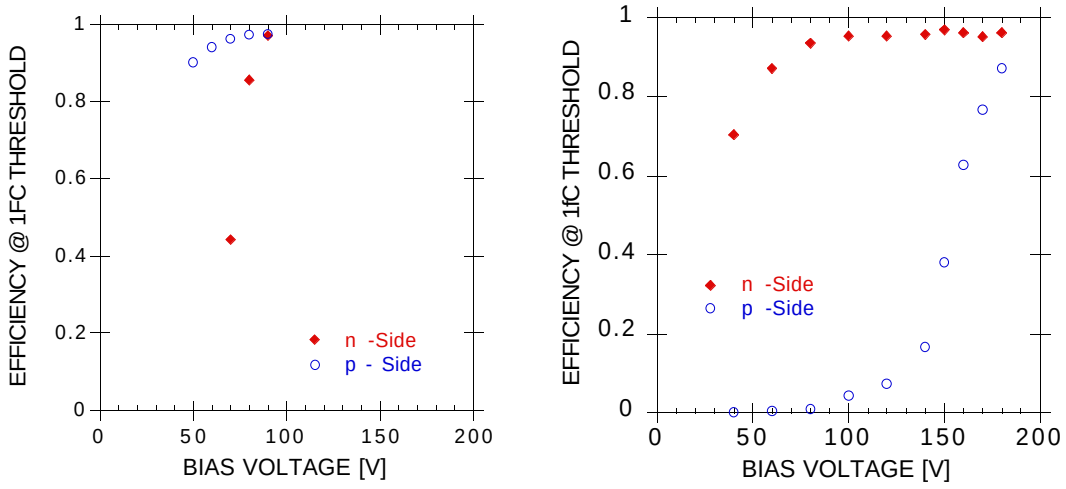

Fig. 5 Efficiency at threshold of 1 fC of a double-sided detector with 50 µm pitch
a) non-irradiated with a depletion voltage of 77V, b) irradiated with depletion voltage 190V (Ref. U2)

The charge sharing in irradiated double-sided detectors has been measured below depletion [R7]. The ratio of (3 hit clusters)/(2 hit clusters) R32 is a measure of the cluster size. The cluster size on inverted double-sided detectors below depletion is shown in Fig. 6. The R32 on the n-side is decreasing with decreasing bias because the collected charge is decreasing and the minimal pulse height considered is fixed at 2σ. On the p-side, R32 is increasing below depletion. This indicates that the charge collected on the p-side is spread over several strips below depletion, and precise localization of the track is not possible.

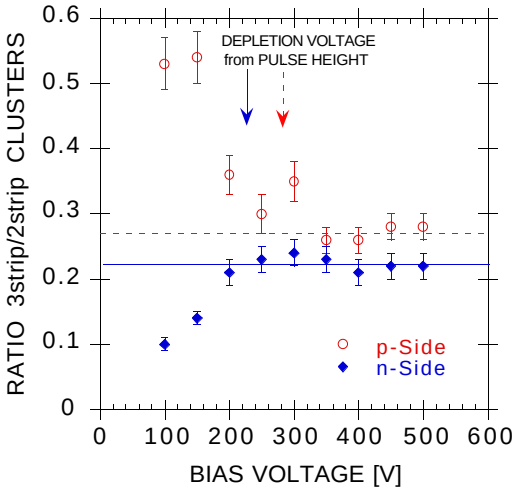

Fig. 6 Ratio of 3 hit clusters to two hit clusters R32 for an irradiated double-sided detector. (Ref. R7)

Because read-out on the junction side allows the detector to be operated under-depleted, n-on-n single-sided detectors function, after inversion, almost as well as before radiation up to much larger fluences than originally anticipated. If the system is designed for a maximum bias voltage of 250V-which by now has been routinely used in several beam tests-it will work with 95% efficiency even if the depletion voltage turns out to be 500V, due to increased luminosity, radiation accidents or possible warm-up. If p-side detectors are used in high radiation conditions, the entire SCT system, power supplies, data transmission, bypassing, cables etc., has to be designed to the largest depletion voltage foreseeable, because changes in the conditions which increase the maximum depletion voltage beyond the anticipated goal strongly reduce the p-side performance.

The fact that n-on-n detectors can be operated under-depleted can be exploited in pixel detectors, which could be operated at a reasonably low bias even in the case of a large depletion voltage [V1-V3]. We have irradiated a single-sided n-on-n detector to 10^{15} p/cm^2, where the depletion voltage is about 2000V, and extracted at 180V bias the pulse height, amounting to 20% of the pre-rad value (Fig. 7). With the very low pixel capacitance, this small a signal charge gives sufficient signal-to-noise for efficient track detection very close to the interaction point.

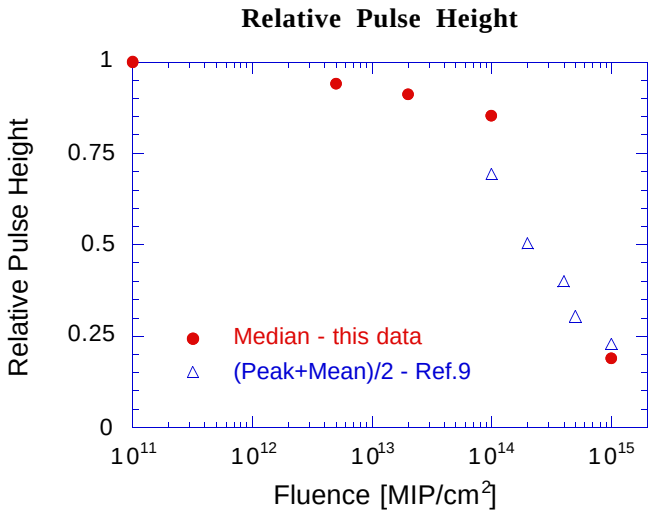

Fig. 7 Relative pulse height of n n-on-n detector at 180 V bias (from Ref. V2. Ref. 9 refers to Ref. V3).

4.2 Noise [Refs. N1, N2]

There is no long-term experience operating heavily irradiated detectors with short shaping times. In laboratory and beam tests, the n-side on irradiated detectors have shown somewhat reduced capacitance and noise with fast shaping front-end electronics (FEE) due to the fact that they have become the junction side (Fig. 8). Laboratory measurements on p-side detectors have shown increased inter strip capacitance and increased noise after radiation [C4].

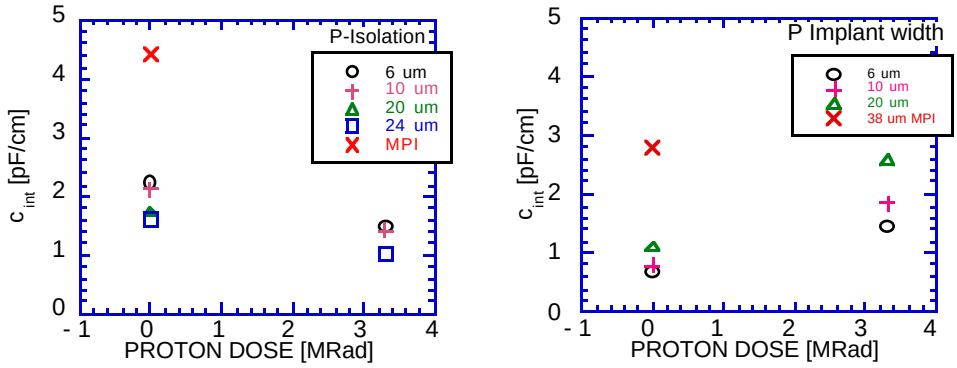

Fig. 8 Inter strip capacitance measurements before and after proton irradiation:
a) n-side, b) p-side (Ref. C4).

Because the amplifier noise depends on the parasitic detector capacitance, the noise performance is directly related to the inter-strip capacitance. The noise occupancy (Fig. 9), *i.e.*, the number of hits per channel per clock-cycle of 25 ns, of irradiated and non-irradiated detectors

agree with the observation that the n-side is the preferred side after heavy irradiation: the occupancy on the n-side is decreased, on the p-side increased.

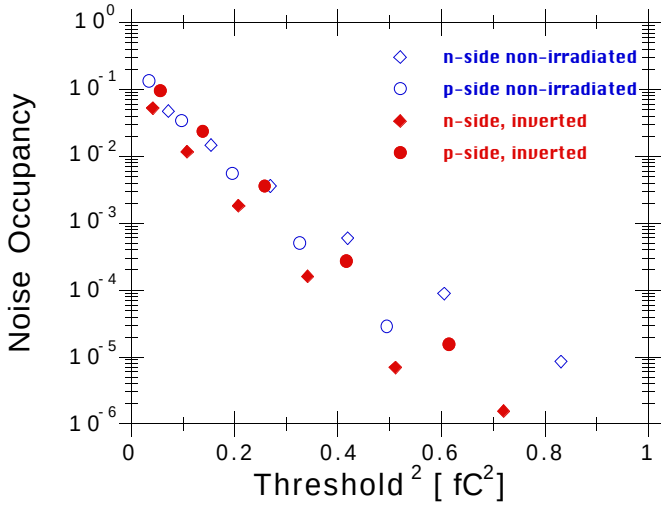

Fig. 9 Noise occupancy as a function of the comparator threshold of non-irradiated and irradiated 6 cm long double-sided detectors (Ref. N2).

4.3 Summary of n- side vs. p-side

The n-on-n detectors have shown good performance with a "head room" of about 20%, when operated close to depletion. This means that the efficiency is almost unchanged when the threshold is increased from 1.0 fC to 1.2 fC. This is due to the high signal-to-noise ratio of about S/N = 15. After radiation damage, the head room can be used to operate under-depleted, if warranted by unforeseen run conditions. At half depletion voltage, the resolution is unchanged and the efficiency is still 95%. The head room is not present for p-side detectors when operated under-depleted: immediately below depletion, the ohmic side looses efficiency and/or resolution. In general, the required bias on the junction side is about half the one needed on the ohmic side.

4.4 Single-sided vs. double-sided detectors

Given that the n-side have superior radiation resistance, the use of the p-side is less advantageous. Indeed, the ATLAS SCT will build sandwiches of two single-sided n-on-n detectors, glued back-to-back, to make a double-sided module. This way the read-out strips and the front-end electronics are at ground, with many advantages for the operation and safety of the detectors at high depletion voltages and the FEE.

4.5 Effect of Glues [Ref. Z2]

We have built and operated in beam tests modules made out of single-sided n-on-n detectors and have seen no adverse effect due to the gluing onto the detector surfaces, either the

ohmic or the junction side, respectively. We have glued hybrids on the front face of silicon modules, either p- or n-side, and operated successfully without increase of noise. One concern is mechanical stresses due to temperature cycling, but for two years, we have operated the modules cold, and they survived a great deal of temperature cycling during beam and bench tests. We have investigated the noise immunity of the sandwich system and find that a noise voltage of 100 mV on the cooling pipe will contribute less than 1/2 noise sigma [H4].

4.6 Cooling [Refs. H1-H3]

The effects of radiation damage can be mitigated by cooling. Both the leakage current and the reverse annealing in the depletion voltage are reduced at low temperatures. But even at operating temperatures of -10^{o}C, the heat conduction in 300 μm thick wafers are not good enough to prevent local heating of the detectors. This can lead to thermal run-away, in case the radiation damage is worse than anticipated or the cooling system not adequate [H1, H2]. The thermal properties of the silicon modules can be vastly improved with the introduction of a "heat spreader", a thin layer of highly thermally conductive material sandwiched between two single-sided detectors which effectively brings the cooling pipe close to the self-heated detector. The ATLAS SCT will use a plane of pyrolytic graphite (PG) which has a heat conductivity close to CVD diamond. Figure 10 shows the principle of the silicon-PG-silicon sandwich, which has been used to investigate the thermal properties of the PG material [H3]. The cooling pipe attaches to one side of the heat spreader only.

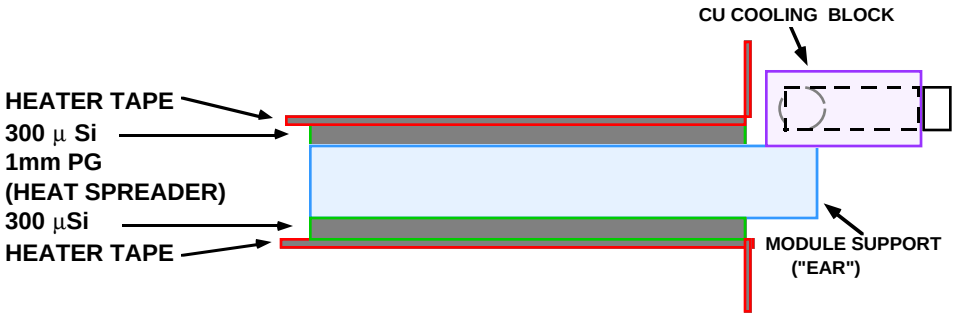

Fig. 10 Cross section through the ATLAS module: a Silicon-PG-Silicon sandwich

A simulation of the temperature distribution across a 12 cm x 6 cm module was performed as a function of the internal heating for both a single wafer module and the Si-PG sandwich. It shows that the Si-PG sandwich allows a factor of at least 3 in the acceptable internal heating before thermal run-away (Fig. 11).

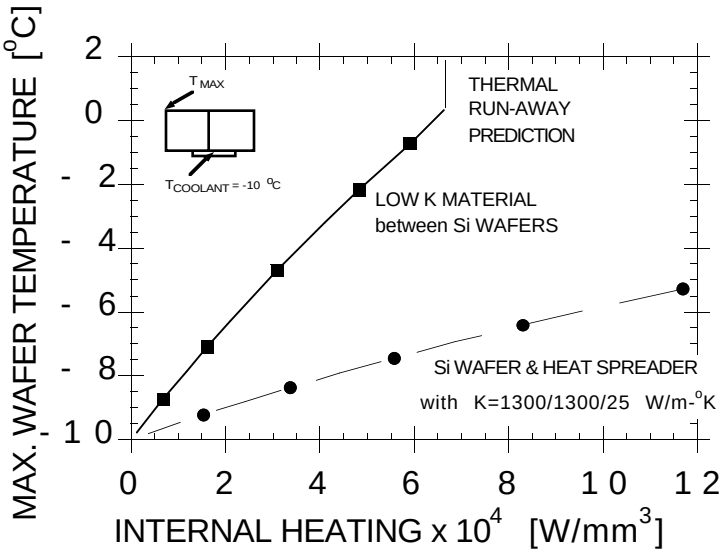

Fig. 11 Simulation of the maximal wafer temperature on a silicon detector with one edge cooled to -10°C as a function of the internal heating. Both a double-sided detector ("Low K") and a Silicon-PG sandwich ("Heat Spreader") are shown (Ref. H3).

The temperature profile across a 6 cm x 12 cm module, both simulated and measured, for a heat input of 3 mW per electronics channel and internal heating of about $2.5*10^{-4}$ W/mm^3 is shown in Fig. 12. The maximum temperature difference on the wafers is of the order of one degree.

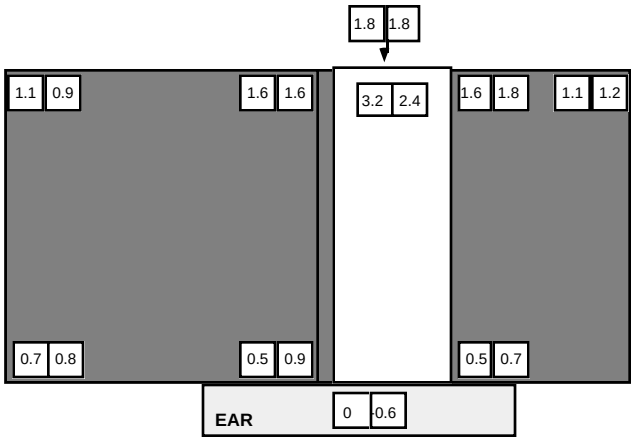

Fig. 12 Measured and simulated temperature profile across a silicon-PG sandwich. Heating occurs both internally and through the FEE (Ref. H3).

5. BEAM TEST RESULTS [Refs. B1-B7]

A series of beam tests have been performed with 12 cm long modules of single-sided n-on-n silicon detectors and fast FEE [B5- B7]. Identical modules were tested in 1996 in the H8 test beam at CERN [B7], with one of them irradiated such that the depletion voltage was 290V,

as determined with C-V measurements (Fig. 13) The detectors were operated cold (at about -10^{o}C) and rotated relative to the beam in a magnetic field of 1.56T to investigate the performance for tracks with crossing angles as expected in the ATLAS detector [T3].

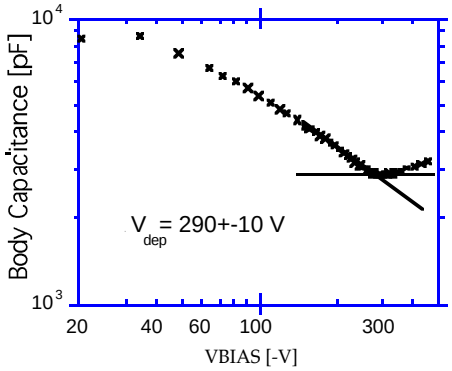

Fig. 13 Determination of the depletion voltage of ATT7, the irradiated 12 cm module, with a C-V curve

The performance is quantified in efficiency and noise occupancy. The noise occupancy is far below 10^{-3} for 1fC threshold. The median pulse height on a single strip and the efficiency at 1fC threshold of the irradiated detector ATT7 both show the slow decrease below the depletion voltage discussed in Sec. 4 (Fig 14). The efficiency of n-on-n detectors is high in the non-irradiated detector when over-depleted (at bias >100V), and in the irradiated detector at 150V which is one half the depletion voltage.

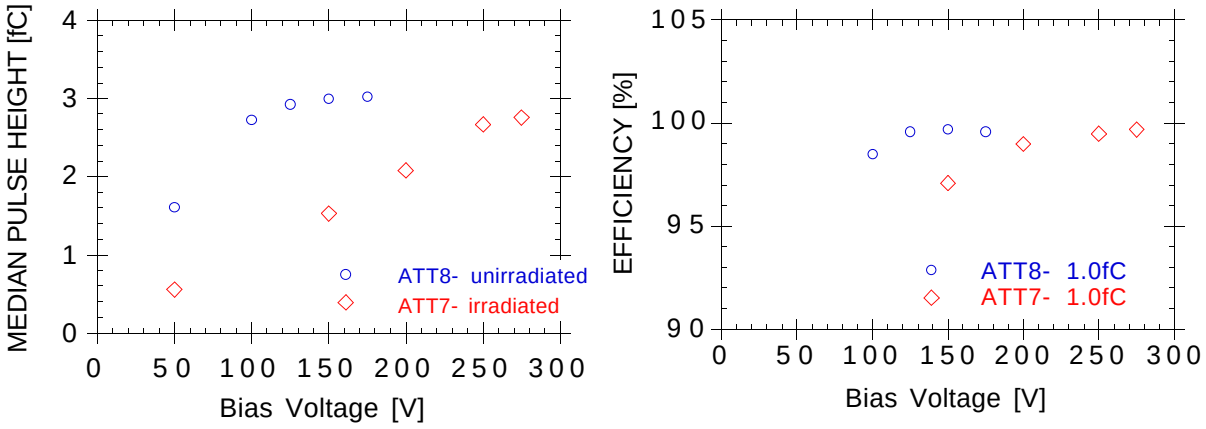

Fig. 14 Bias voltage dependence of 12 cm n-on-n modules ATT8 and irradiated ATT7 (depletion voltage 290V):
a) median pulse height, b) efficiency at 1fC threshold (Ref. B7).

For the rotated detectors in a magnetic field, the efficiency is independent of rotation angle for the required range of ±15^{o} relative to the anticipated tilt angle of about +10^{o} (Fig 15a). When biased at 1/2 the depletion voltage, the efficiency of the irradiated detector ATT7 is still 95% at 1.0 fC threshold. It turns out that biased at the full depletion voltage, the efficiency is

high even at a threshold of 1.2 fC, 20% higher than the threshold required for noise suppression [B7]. The position resolution of the irradiated detector identical to the non-irradiated one (Fig. 15b). It is constant as a function of rotation angle and close to the expected value of pitch/√12. At 1/2 the depletion voltage, the position resolution for ATT7 is the same as at full depletion.

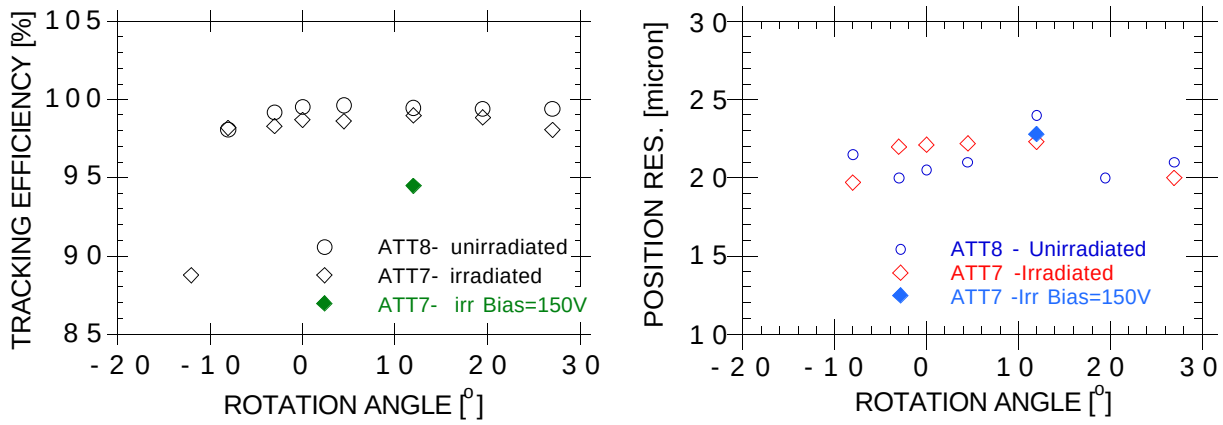

Fig. 15 Rotation angle dependence in a 1.56T magnetic field with bias at 250V (ATT7) and 125V (ATT8): a) efficiency at 1fC threshold, b) position resolution (Ref. B7).

As mentioned in Sec. 3, short-term radiation effects can effectively be understood only in realistic operating conditions. For part of the runs, the intensity of the test beam was increased to the instantaneous flux expected for operation at the LHC. As mentioned before, the detectors were cooled to -10°C throughout the beam test. No change in efficiency was observed neither for the non-irradiated nor the inverted module (Fig. 16).

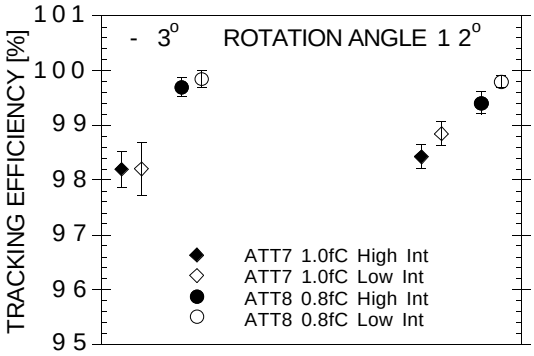

Fig. 16 Efficiency for both irradiated (ATT7) and unirradiated (ATT8) module during high and low intensity running for two rotation angles.

6. CONCLUSIONS

For the ATLAS silicon tracker, a sandwich of single-sided n-on-n detectors was chosen as the base line, because their superior performance after heavy radiation damage has been proven over the last years. They exhibit good signal-to-noise ratio, even when operated under-depleted after radiation induced inversion. The alternative, double-sided detectors, has been shown to require full depletion on the p-side. In several beam tests, fully instrumented modules have been operated, some of them irradiated with realistic LHC fluences. The results confirm that the single-sided n-on-n detector affords the performance head room required for the high radiation environment of ATLAS and the uncertainty in predicting the operating conditions. With n-on-n detectors, the ATLAS SCT will be able to survive either higher radiation levels than anticipated or unexpected scenario's of warming up of the detectors, and will be able to profit from a more optimistic luminosity scenario.

7. ACKNOWLEDGMENTS

The development of silicon detectors for high luminosity application has been a world-wide effort. I would like to acknowledge the collaboration with many people. I would like to thank the staff of the SCIPP Microelectronics laboratory for their excellent work. This work has been supported by the US Department of Energy.

8. REFERENCES

Annealing

[A1] H. Ziock *et al.*, Temperature Dependence of the Radiation Induced Change of Depletion Voltage in Silicon PIN Detectors, Nucl. Instrum. Methods **A342**, 96 (1994) (http://scipp.ucsc.edu/~hartmut/Hiro.mod.ps).

[A2] E. Frettwurst *et al.*, Reverse Annealing of the Effective Impurity Concentration and Long Term Operational Scenario for Silicon Detectors in Future Collider Experiments, Nucl. Instrum. Methods **A342,** 119 (1994).

[A3] H. F.-W. Sadrozinski, Depletion Voltage and short-term Annealing, SCIPP 96/57 (http://scipp.ucsc.edu/~hartmut/Dep_Volt_ALL.paper.ps).

Beam Tests

[B1] Y. Unno *et al.*, Beam Test of the SDC Double-sided Silicon Strip Detector, presented at the 1993 IEEE Nucl. Sci. Symp., KEK 93-127, (http://arkhp1.kek.jp/~unno/notes/BeamtestIEEE93.ps).

[B2] J. DeWitt *et al.*, Signal-to-Noise in Silicon Microstrip Detectors with Binary Readout, IEEE Trans. N.S. **42**, 445 (1995), (http://scipp.ucsc.edu/groups/silicon/papers/ieee94.w3.ps).

[B3] Y. Unno *et al.*, Beam Tests of a Double-sided Silicon Strip Detector with Fast Binary Readout Electronics Before and After Proton Irradiation, Nucl. Instrum. Methods **A383,** 211 (1996), (http://arkhp1.kek.jp/~unno/notes/BeamtestSiSymp95.ps).

[B4] J. Beringer *et al.*, ATLAS Beam Test Results, Nucl. Instrum. Methods **A383,** 205 (1996).

[B5] J. DeWitt *et al.*, Test Results of Silicon Micro-strip Detectors for ATLAS, subm. to 5th Int. Workshop on Vertex Detectors, Chia, Italy, June 1996, SCIPP 96/25, (http://scipp.ucsc.edu/groups/silicon/preprints/vertex96.ps).

[B6] Y. Unno *et al.*, Beam Test of a large Area n-on-n Silicon Strip Detector with Fast Binary Readout Electronics, IEEE Nucl. Sci. Symp., Nov. 3-8, 1996, Anaheim, CA, (http://arkhp1.kek.jp/~unno/notes2/IEEE96shortV2.2.ps).

[B7] F. Albiol *et al.*, Beam Test of the ATLAS Silicon Detector Modules with Binary Readout in the CERN H8 Beam in 1996, SCIPP 96/49 (http://scipp.ucsc.edu/~hartmut/H8_96_trans.ieee.ps).

Interstrip Capacitance , Simulations

[C1] R. Sonnenblick, A 2-dim Simulation of a Silicon Microstrip Detector, UC Santa Cruz Physics Dept. Senior Thesis 1995, SCIPP 90/21.

[C2] R. Sonnenblick *et al.*,, Electrostatic Simulations for the Design of Silicon Strip Detectors and Front-end Electronics, Nucl. Instrum. Methods **A310**, 189 (1991).

[C3] S. Gadomski *et al.*, Pulse Shapes of Silicon strip Detectors as a Diagnostic Tool, Nucl. Instrum. Methods **A326**, 239 (1993).

[C4] E. Barberis *et al.*, Capacitances in Silicon Microstrip Detectors, Nucl. Instrum. Methods **A342**, 90 (1994).

[C5] J. Leslie, A. Seiden and Y. Unno, Signal Simulations of Double-sided Strip Detectors for the SSC, IEEE Trans. Nucl. Sci. **40**, 557, (1993), (http://scipp.ucsc.edu/~hartmut/ATLAS/SIGSIM).

Silicon Detectors

[D1] M. Turala, Silicon Microstrip Detectors, DPF Conference 1985, Eugene, OR.

[D2] T. Ohsugi *et al.*, Double-sided Microstrip Sensors for the Barrel of the SDC Silicon Tracker, Nucl. Instrum. Methods **A342,** 16 (1994).

[D3] A. Litke and A. Schwarz, The Silicon Microstrip Detector, Scientific American **272**, 56 (May 1995).

Front-end Electronics

[E1] J. DeWitt, The Digital Time Slice Chip, UC Santa Cruz Physics Dept. Senior Thesis 1988, SCIPP 88/23.

[E2] D. Dorfan, Bipolar Front-end Amplifier for Use with Silicon Strip Detectors, Nucl. Instrum. Methods **A342,** 143 (1994).

[E3] E. Barberis *et al*, Design, Testing and Performance of the Front-end Electronics for the LPS Silicon Microstrip Detectors, Nucl. Instrum. Methods **A364,** 507 (1995) (http://scipp.ucsc.edu/groups/silicon/papers/LPS.elec.6.ps).

[E4] E. Spencer *et al.*, A Fast Shaping Low-Power Amplifier-Comparator Integrated Circuit for Silicon Strip Detectors, IEEE Trans Nucl. Sci. **42**, 796 (1995), (http://scipp.ucsc.edu/groups/silicon/papers/LBIC.ps).

[E5] J. DeWitt, A Pipeline and Bus Interface Chip for Silicon Strip Detector Readout, IEEE Nucl. Sci. Symp., San Francisco, CA, Nov. 1993, SCIPP 93/37, (http://scipp.ucsc.edu/groups/silicon/papers/CDP128.ps).

[E6] K. Shankar *et al*, Digital Read-out Chip for Silicon Strip Detectors at SDC, IEEE Trans. Nucl. Sci. **42**, 792 (1995).

[E7] I. Kipnis, CAFE, A Complementary Bipolar Analog Front-end Integrated Circuit for the ATLAS SCT, unpublished.

[E8] A. Ciocio *et al.*, A Binary Readout System for Silicon Strip Detectors at the LHC, Presentation at the LHC Electronics Workshop, Lisbon, Portugal, Sept. 12, 1995.

[E9] W. Dabrowski, Development of Readout Chips for the ATLAS Semiconductor Tracker, Nucl. Instrum. Methods **A383,** 179 (1996).

LHC Fluences

[F1] A. Van Ginneken, Non-ionizing Energy Deposition in Silicon for Radiation Damage Studies, Fermilab Preprint FN522 (1989).

[F2] G. Gorfine and G. Taylor, Particle Fluxes and Damage to Silicon in the ATLAS Inner Detector, Univ. of Melbourne Preprint UM-P-93/103, 1993.

[F3] G. W. Gorfine, Studies of Radiation Levels in the LHC and of Radiation Damage to Silicon Detectors, U. of Melbourne PhD Thesis, 1994.

[F4] J. Matthews *et al*, Implications of Different Operating Temperatures and Maintenance Scenarios for the ATLAS SCT, ATLAS INDET Note 128.

Heat Management, Cooling

[H1] W. O. Miller *et al.,* Thermal Run-away in Silicon Strip Detectors, SCIPP 94/43.

[H2] T. Kohriki *et al.*, Observation of Thermal Runaway, IEEE Trans. Nucl. Sci. **43**, 1200 (1996).

[H3] W. O. Miller *et al.,* The SPGS Module, Thermal Measurements and Simulations with a Silicon Detector - PG Sandwich, IEEE N. S. Symp., Nov. 3-8, 1996, Anaheim, CA, SCIPP 96/52, (http://scipp.ucsc.edu/~hartmut/spgs.ieee.ps).

[H4] T. Dubbs and H. F.-W. Sadrozinski, Silicon Detector Noise Coupled in from the Cooling Pipe, SCIPP 96/64, (http://scipp.ucsc.edu/~hartmut/Pipe_Noise.ps).

Type Inversion

[I1] D. Pitzl *et al.*, Type Inversion in Silicon Detectors, Nucl. Instrum. Methods **A311,** 98 (1992).

LHC Detectors

[L1] A Toroidal LHC Apparatus ATLAS Technical Proposal, CERN/LHCC/94-43.

[L2] The Compact Muon Solenoid CMS Technical Proposal, CERN/LHCC/94-38.

[L3] A Large Ion Collider Experiment ALICE Letter of Intent, CERN/LHCC/93-16.

Noise

[N1] T. Pulliam, Noise Studies in Silicon Micro strip Detectors, UC Santa Cruz Physics Dept. Senior Thesis 1995, SCIPP 95/28, (http://scipp.ucsc.edu/groups/silicon/papers/noise_thesis.ps).

[N2] T. Dubbs *et al.*, Noise Determination in Silicon Microstrip Detectors, IEEE Trans. Nucl. Sci. **43**, 1119 (1996), (http://scipp.ucsc.edu/groups/silicon/preprints/IEEE95_noise.ps).

Radiation Damage

[R1] P. Giubellino *et al*, Study of the Effects of Neutron Irradiation on Silicon Strip Detectors, Nucl. Instrum. Methods **A315,** 156 (1992).

[R2] H. F.-W. Sadrozinski *et al.*, Limits to the Use of Irradiated Silicon Detectors, SCIPP 94/06.

[R3] J. Matthews *et al.,* Bulk Radiation Damage in Silicon Detectors and Implications for LHC Experiments, Nucl. Instrum. Methods **A381,** 338 (1996).

[R4] G. N. Taylor *et al*, Radiation Induced Bulk Damage in Silicon Detectors, Nucl. Instrum. Methods **A383,** 144 (1996).

[R5] S. Terada *et al*, Proton Irradiation on p-bulk Silicon Strip Detectors Using 12GeV PS at KEK, Nucl. Instrum. Methods **A383,** 159 (1996).

[R6] C. Leroy *et al*, Study of Charge Collection and Noise in Non-irradiated and Irradiated Silicon Detectors, CERN-ECP/96-05.

[R7] P. Allport, J. Carter *al.*, ATLAS Radiation Damage Study on Single- and Double-sided Silicon Strip Detectors, Dec. 1996, private communication.

[R8] E, Borchi, M. Bruzzi and M. S. Mazzoni, Thermally Stimulated and Leakage Current Analysis of Neutron Irradiated Silicon Detectors, Nucl. Instrum. Methods **A310,** 273 (1991).

Surface Damage

[S1] D. Pitzl *et al..*, Study of Radiation Effects on AC-coupled Silicon Strip Detectors, Nucl. Physics B (Proc. Suppl.) **23A**, 340 (1991).

[S2] R. Weaton, Radiation Tolerance Studies of Silicon Microstrip Detectors for the LHC, Nucl. Instrum. Methods **A342,** 126 (1994).

[S3] N. Bacchetta *et al.*, FOXFET Biased Microstrip Detectors: an Investigation of Radiation Sensitivity, Nucl. Instrum. Methods **A342,** 39 (1994).

[S4] R. Wunstorf *et al.*, Damage-induced Surface Effects in Silicon Detectors, Nucl. Instrum. Methods **A377,** 290 (1996).

[S5] T. Ohsugi *et al.*, Micro-discharge Noise and Radiation Damage of Silicon Microstrip Sensors, Nucl. Instrum. Methods **A383,** 166 (1996).

[S6] P. Azzi *et al.*, Radiation Damage Experience at CDF with SVX', Nucl. Instrum. Methods **A383,** 155 (1996).

Layout issues

[T1] H. F.-W. Sadrozinski, A. Seiden and A. Weinstein, Tracking at 1TeV, Nucl. Instrum. Methods **A277** 92 (1989).

[T2] ATLAS SemiConductor Tracker SCT, ATLAS INDET Note 085 (1995).

[T3] H. F.-W. Sadrozinski, Tilt Angle, Crossing Angle and Lorentz Angle, SCIPP 96/48.

[T4] P. Collins, Experience with Silicon Detectors at the DELPHI Experiment, Nucl. Instrum. Methods **A383** 1 (1996).

[T5] R. P. Johnson, BaBar Silicon Vertex Tracker, Nucl. Instrum. Methods **A383** 7 (1996).

Non-uniformly irradiate d detectors

[U1] M. Schwab, Characterization of Silicon Strip Detectors with ^{106}Ru, UC Santa Cruz Physics Dept. Senior Thesis 1995, SCIPP 95/29.

[U2] T. Dubbs *et al.*, Efficiency and Noise Measurements of Non-uniformly Irradiated Double-sided Silicon Strip Detectors, Nucl. Instrum. Methods **A383,** 174 (1996), (http://scipp.ucsc.edu/groups/silicon/preprints/hirosh.ps).

[U3] Y. Unno *et al.*, Characterization of an Irradiated Double-sided Silicon Strip Detector with Fast Binary Readout Electronics in a Pion Beam, IEEE Trans. Nucl. Sci. **43**, 1175 (1996), (http://arkhp1.kek.jp/~unno/notes/IEEE95paper5.ps).

[U4] A. Gomez, Determination of the Depletion Voltage of non-uniformly irradiated Silicon Microstrip Detectors, UC Santa Cruz Physics Dept. Master Thesis 1997, SCIPP 97/05.

Very High Fluence

[V1] I. Abt *et al.*, Irradiation Tests of Double-sided Silicon Detectors with a special Guard Ring Structure, IEEE Trans. Nucl. Sci. **43**, 1113 (1996).

[V2] A. Gomez *et al.*, Pulse Height of an n-side Silicon Microstrip Detector after Proton Irradiation with a Fluence of $1*10^{15}$p/cm^2, SCIPP 96/42, (http://scipp.ucsc.edu/~hartmut/LBL_Irr.paper.ps).

[V3] R. Horisberger *et al.*, presented at the 3rd International Workshop on Pixel Detectors for Particles and X-Rays, Bari, Italy, March 1996.

Assembly, Testing

[Z1] E. Barberis *et al.*, A Test station for Silicon Microstrip Detectors and Associated Electronics, The Fermilab Meeting, DPF-92, vol. 2, 1752 (1992).

[Z2] O. Runolfson, Quality Assurance and Testing Before, During, and After Construction of Semiconductor Tracking Detectors, Nucl. Instrum. Methods **A383**, 223 (1996).